

There are a number of medicines for the treatment of inflammatory bowel diseases available in the clinic as solid dosage forms coated with Eudragit S. Those available in the UK include Asacol[®] MR (Procter and Gamble), Mesren MR[®] (Teva), Ipcol[®] (Sandoz) and Budenofalk[®] (Dr Falk). The first three products contain the anti-inflammatory agent mesalazine (mesalamine, 5-aminosalicylic acid) and the last contains the corticosteroid budesonide.

Eudragit S coated dosage forms display different *in vitro* and *in vivo* release profiles. *In vivo*, these formulations have been reported to dissolve prior to reaching the ileo-colonic region or even traversing the entire GI tract intact with no observed dissolution.¹ While products have the same Eudragit S polymer in their coating, different plasticizers can influence dissolution.⁵ Moreover, *in vivo* performance is further complicated by the complexity of the GI tract. This includes inter- and intra-individual variations in pH, limited fluid availability in the distal gut⁶ and variations in transit times, which can be magnified by food.⁷

As a free flowing dry powder, Eudragit S has a high glass transition temperature (433–444 K). To produce Eudragit S film coatings, it is essential to blend this polymer with a plasticizer to reduce coating brittleness and to achieve smooth, crack-free coatings. A miscible plasticizer increases film flexibility by reducing intermolecular interactions between individual polymer molecules;⁸ this can influence drug release.⁹ It has been proposed that plasticizer enhancement of polymer mobility alters the distribution of diffusion channels and therefore drug diffusion through the water-insoluble polymer systems.¹⁰ However studies have not substantiated this.¹¹ Our objective is to correlate the dielectric response with dissolution of Eudragit S blended films. This may enable us to tailor coating formulations and processing to achieve an optimal drug release profile within the ileo-colonic region of the GI tract. Since inflammatory bowel diseases affect various regions in the distal gut, it is hoped that treatment options may eventually include medicines where release occurs at tissue sites affected by disease.

In this work we have conducted a comparative study of the dielectric properties of plasticized Eudragit S solvent cast films by thermally stimulated depolarization current (TSDC) spectroscopy. Films derived from four citrate plasticizers ranging from very low to moderate aqueous solubility were examined. TSDC is a rather novel technique for pharmaceutical material characterization. It relies

on dipolar rearrangements to generate depolarization currents that can be related to local (secondary relaxations) and cooperative (structural relaxations) molecular mobilities. Its high sensitivity and low equivalent frequency (~1 mHz) leads to an enhancement of the resolution of the coexisting dipolar processes.¹² Multicomponent peaks can then be resolved accurately to correlate the individual molecular motions with their dielectric relaxations.¹³ The glass transition (T_g) temperature that was determined by TSDC was also compared to the T_g which was determined by differential scanning calorimetry (DSC) and dynamic mechanical analysis (DMA).

MATERIALS AND METHODS

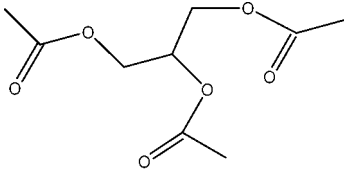
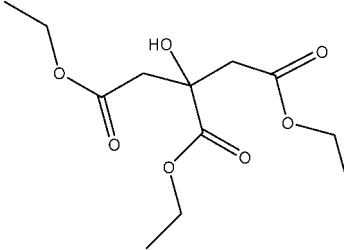
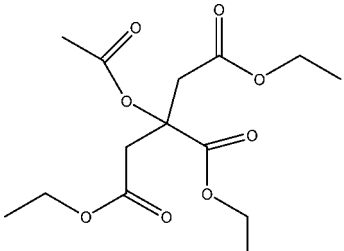
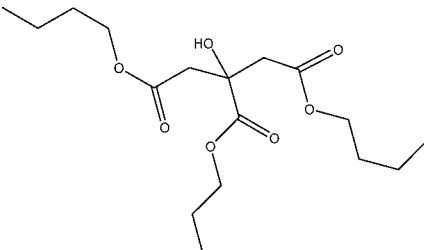
Materials

Eudragit S polymer (MW = 135000 g/mol) was donated by Evonik. Four plasticizers were examined (Tab. 1). The plasticizers triacetin (TA) and acetyl triethyl citrate (ATEC) were purchased from Sigma–Aldrich, Gillingham, UK. Triethyl citrate (TEC) and tributyl citrate Gillingham (TBC) were purchased from Fluka, Seelze, Germany.

Film Fabrication

Cast films were fabricated from polymer–plasticizer solutions in ethanol by solvent evaporation. The plasticizer, 15% or 20% of polymer weight was first dissolved in 100 g of 95% ethanol for 30 min at room temperature in a beaker. Eudragit S powder (8.5% w/w of solvent) was gradually added to the ethanolic solution that was rapidly stirred by a Heidolph RZR1 overhead stirrer at a speed of 500 rpm. The mixing vessel was sealed with Parafilm to prevent solvent evaporation and the solution was stirred for a further 12 h to ensure the polymer had dissolved. A portion of the solution (9 mL) was poured onto separate Teflon[®] moulds (9 cm diameter) and allowed to dry at room temperature for 8 h. The films were then peeled from the Teflon moulds and placed in an oven at 50°C for 48 h to remove residual ethanol/water. Two water-soluble plasticizers were examined at a 20% w/w concentration based on polymer weight: (1) triacetin (TA) and (2) triethyl citrate (TEC). Their solubility in water (%m/v) is 6.7–7.8% and 5.5–6.9% respectively. Acetyl triethyl citrate (ATEC) has a lower water solubility of 0.72% and was also included at a 20% w/w concentration. Tributyl citrate (TBC), the fourth additive has a

Table 1. Structure, Molecular Weight (MW) and Water Solubility of Plasticizers Used in This Study

Plasticizer	Structure, g/mol MW	% m/v Water Solubility
Triacetin (TA)	 MW 218	6.7–7.8
Triethyl citrate (TEC)	 MW 276	5.5–6.9
Acetyl triethyl citrate (ATEC)	 MW 318	0.72
Tributyl citrate (TBC)	 MW 360	<0.002

much lower water solubility (less than 0.002%) and could only be included at a concentration of 15% of polymer weight before phase separation was observed. Plasticizer content in the films was confirmed using $^1\text{H-NMR}$ (Bruker Avance 500 MHz NMR spectrometer). Film thickness was measured at different points using a micrometer (Mitutoya, Japan) and was found to be $130 \pm 10 \mu\text{m}$. The films were subsequently stored under vacuum in a desiccator.

Film Dissolution

Film dissolution was measured using a custom made two-compartment permeation cell. A sample film with an area of 1.8 cm^2 separated the two compartments with the aid of an O-ring separation. The film was incubated at pH 7.4 in phosphate buffer (0.05 M) under sink conditions. The donor compartment had a volume of 5 mL and was filled with a saturated solution of the drug

mesalazine (6.34 mg/mL) in pH 7.4 phosphate buffer. The acceptor compartment also had a volume of 5 mL, however continuous flow was employed in this compartment whereby a volume of 100 mL of pH 7.4 phosphate buffer (0.05 M) maintained at 37°C was circulated through *via* a peristaltic pump. The solution in the acceptor compartment was continuously stirred using a magnetic stirrer. Mesalazine was selected as the model drug as it is commonly used in the treatment of inflammatory bowel diseases. Onset of mesalazine permeation from the donor to the acceptor compartment was determined by UV spectrophotometry at 330 nm and was found to correspond to film dissolution as pores in the film became clearly visible. UV readings were taken automatically every 15 min by an in-line UV spectrophotometer (Cecil 2020, UK). Phosphate buffer continuously circulated through the acceptor compartment passed through the UV-spectrophotometer so that UV measurements were taken in real time. All film formulations were tested in triplicate.

Thermally Stimulated Depolarization Currents

The principle of the thermally stimulated depolarization current (TSDC) technique is based on the strong dependence of the dielectric relaxation time, τ , on temperature T . A sample is polarized in an electric field (typically 5×10^5 V/m) and the state of polarization is frozen by quenching the sample rapidly (55 K min^{-1}) to liquid nitrogen temperature. The electric field is then switched off and the sample temperature is increased at a controlled rate (0.1 K s^{-1}) to record the depolarization current caused by the disorientation of the dipoles. A Cary Vibrating Reed Electrometer (Model 401) is used to record the depolarization current. The sensitivity of our current measuring system is 10^{-17} A and the signal to noise ratio is greater than 500. The current-temperature data acquisition is fully automatic.

To characterize the temperature region of the dielectric spectra two consecutive experimental cycles were performed on the samples. The first cycle consists of a thermally stimulated polarization current (TSPC) experiment. The TSPC method consists in lowering the sample temperature from 300 K to liquid nitrogen temperature at a rate of approximately 1 K s^{-1} . At this point a polarizing field is applied to the sample while it is simultaneously heated at a rate of 0.1 K s^{-1} . The

polarization current versus temperature is digitally recorded. At high temperatures, the glass transition peak is followed by a step increase due to the conductivity of the polymer; at this stage the first cycle is concluded. Henceforth, without removing the external field, the temperature of the sample is lowered back again to liquid nitrogen at a rate of approximately 1 K s^{-1} to begin the second cycle or to begin a TSDC experiment. When the sample again has reached liquid nitrogen temperature, the polarizing field is removed and the temperature is raised at a rate of 0.1 K s^{-1} while the depolarization current is detected. Further details of the TSDC method have been described elsewhere.¹² All measurements were obtained at least in triplicate.

Analysis of TSDC Results

Direct signal analysis (DSA) is a curve-fitting procedure that was developed to analyze the complex low temperature TSDC peaks.¹⁴ The method consists of finding the elementary curves whose characteristic energies are equally spaced in a given energy window and whose combination best fits the whole experimental TSDC profile. The recorded TSDC current is approximated by Eq. (1).

$$J_D(T_j) = \sum_{i=1}^N \frac{P_{0i}}{\tau_i(T_j)} \exp\left(-\frac{1}{b_h} \int_{T_0}^{T_j} \frac{dT'}{\tau_i(T')}\right), \quad (1)$$

with $j = 1, M$; $N \leq M/2$

The relaxation time for each elementary process is $\tau(T)$, its contribution to the total polarization is P_{0i} , and the heating rate is b . The temperature dependence of the relaxation time of the low temperature relaxations can be represented by the Arrhenius expression, Eq. (2).

$$\tau_i(T) = \tau_{0i} \exp(E_{0i}/kT) \quad (2)$$

where τ_{0i} and E_{0i} are the pre-exponential and the reorientation energy of the i elementary curve respectively. The DSA method adjusts $J_D(T)$ (Eq. 1) to the experimental data using the Marquardt–Levenberg nonlinear least-squares fitting algorithm.

To characterize the glass transition relaxation a model was used that assumes a dipolar system having been formed by permanent electric dipole moments that are fixed to the mobile polymeric chains.¹⁵ With this model using the

Williams–Landel–Ferry, WLF, zero order approximation for the temperature dependence of $\tau(T)$, for the case where $T \sim T_g$ or when the free volume fraction coefficient is large,^{16,17} it is possible to express the thermally stimulated depolarization current as a function of T :

$$J(T) = J_0 \frac{\exp(\beta(T - T_g))}{\exp(\eta(T - T_g)/T) + 1} \quad (3)$$

where J_0 is the current density amplitude; β is the zero order approximation near the glass transition temperature of the WLF, T_g is the measured glass transition temperature of the relaxation; and η includes the contribution of the dipolar energy as well as the energy from the polymeric matrix.¹⁵ To analyze the glass transition relaxation peaks obtained from the TSDC experiments with Eq. (3), we use a standard nonlinear algorithm plus a search region for some of the parameters to make sure that an absolute minimum is obtained for the least mean square deviations between expression (3) and the data analyzed.

Dynamic Mechanical Analysis

Dynamic mechanical analysis (DMA) was conducted using a Tritec 2000 DMA (Triton Technology Ltd., Nottinghamshire, UK). Films were cut into dimensions of 6 mm width and 2 mm length and subjected to a tensile deformation mode at a frequency of 1 Hz, static preload of 0.1 N and dynamic displacement of 10 μm . A heating rate of 6 K/min was employed from 298 to 473 K. The T_g value is reported as the peak loss modulus as opposed to the peak $\tan \delta$. The former is the more appropriate representation as the upper temperature for use of most amorphous polymers is their ‘softening point.’ Hence by the transition midpoint (peak $\tan \delta$) this softening point would have been exceeded.¹⁸ All measurements were obtained at least in triplicate.

Differential Scanning Calorimetry

Film samples were evaluated by differential scanning calorimetry (DSC) using a Pyris 1 instrument (PerkinElmer Instruments, Bucks, UK). StepScan-DSCTM (SSDC) was employed; this performs relatively fast, repetitive sequences of short heat-hold segments. This differs from modulated DSC in that it uses an isothermal step instead of a cooling step. The sample was heated at 6 K min⁻¹ for 2 K increments and then allowed to equilibrate for 0.5 min before being subjected to

heating again. The sample was scanned from 298 to 473 K with a nitrogen gas purge at a flow rate of 20 mL/min. The T_g was taken as the half change in specific heat capacity (C_p) of the sample. All measurements were conducted at least in triplicate. Calibration was performed at a heating rate of 6 K min⁻¹ using the standard references, indium and lead.

Thermogravimetric Analysis

Thermogravimetric analysis (TGA) was performed with a Perkin–Elmer Pyris 6 TGA using 8–13 mg of film at a scan rate of 10 K min⁻¹ over a temperature range of 303–423 K. After storage under vacuum the residual solvent of the films was in the range of 0.63–1.84% of sample mass. All measurements were conducted at least in triplicate.

RESULTS

Dissolution onset times of the films are shown in Figure 1. Four films each incorporating a citrate-based plasticizer (TBC, ATEC, TEC, or TA) and a control film with no plasticizer were evaluated. Except for TBC where phase separation was observed during film fabrication, the concentration of plasticizer used was 20% w/w with Eudragit S. Hence, to examine TBC, we used it at 15% w/w. Compared to Eudragit S alone (EU), which has a dissolution onset of 9.25 ± 1.02 h, the slowest film to dissolve was EU-TBC at 19.0 ± 1.82 h. This additive is the least water soluble of the plasticizers that were evaluated (<0.002% m/v H₂O).¹⁹ The dissolution times for the other three blended films were faster than for Eudragit S alone. The aqueous solubility of ATEC (0.72% m/v H₂O)

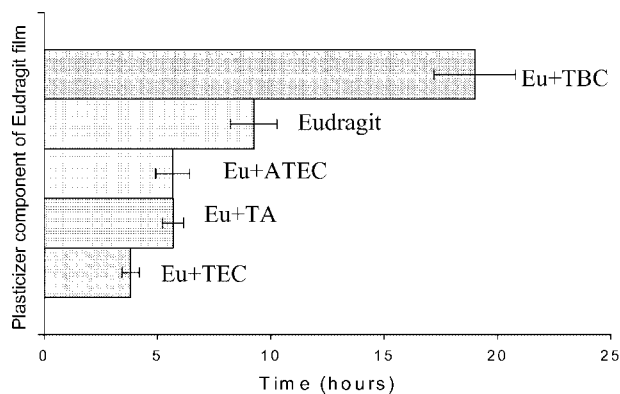


Figure 1. Onset of dissolution of Eudragit S films with and without plasticizers. Mean values \pm SD.

is about 10 times less than TA (6.7–7.8% m/v H₂O) and TEC (5.5–6.9% m/v H₂O), and the respective dissolution times of their films were 5.67 ± 0.75 , 5.69 ± 0.46 and 3.81 ± 0.38 h (Fig. 1).

Dielectric spectra are shown in Figure 2A–C. The dielectric processes in the low and high temperature regions for the Eudragit S film are shown in Figure 2A. These data (Fig. 2A) were obtained by conducting two consecutive cooling-warming cycles (TSPC followed by TSDC). The polarization field was maintained during the first heating cycle (TSPC) and then removed during the second heating cycle (TSDC). Secondary relaxation processes occur in the temperature range from 80 to 300 K. The dielectric manifestation of the glass transition appears (peak α) in the higher temperature range from 300 to 440 K.

The low temperature TSDC dielectric spectra for all the solvent cast films are shown in Figure 2B. Polarization was conducted at 300 K. The low temperature zones (80–310 K) in Figure 2B display broad multi-component peaks, with the EU-ATEC film displaying the most intense peak. Compared to the Eudragit S film, the maximum for this broad band had shifted to slightly higher temperatures for all the plasticized films. The high temperature dielectric spectra are shown in Figure 2C and were obtained after polarizing the samples at the maximum of each α peak. The temperature position of the α peaks was obtained from experimental cycles similar to the ones shown in Figure 2A. The α peaks (Fig. 2C) of the blended films displayed a lower temperature than that observed for Eudragit S alone. Amongst the blended films, there were different temperature maxima and signal intensities. Comparative glass transition temperatures (T_g) were obtained by DSC (Fig. 3) and by DMA (Fig. 4). These T_g values along with the residual solvent values obtained by TGA are listed in Table 2.

DISCUSSION

The dissolution times for the films are shown in Figure 1. TSDC was used to compare the dielectric properties of each film to attain a better understanding of the molecular interactions between the plasticizer and Eudragit S that may influence film dissolution. The complex TSDC spectra presented in Figure 2A are composed of several overlapping and non mono-energetic peaks that cannot be described by assuming an elementary Debye process.²⁰ Deconvolution is required to

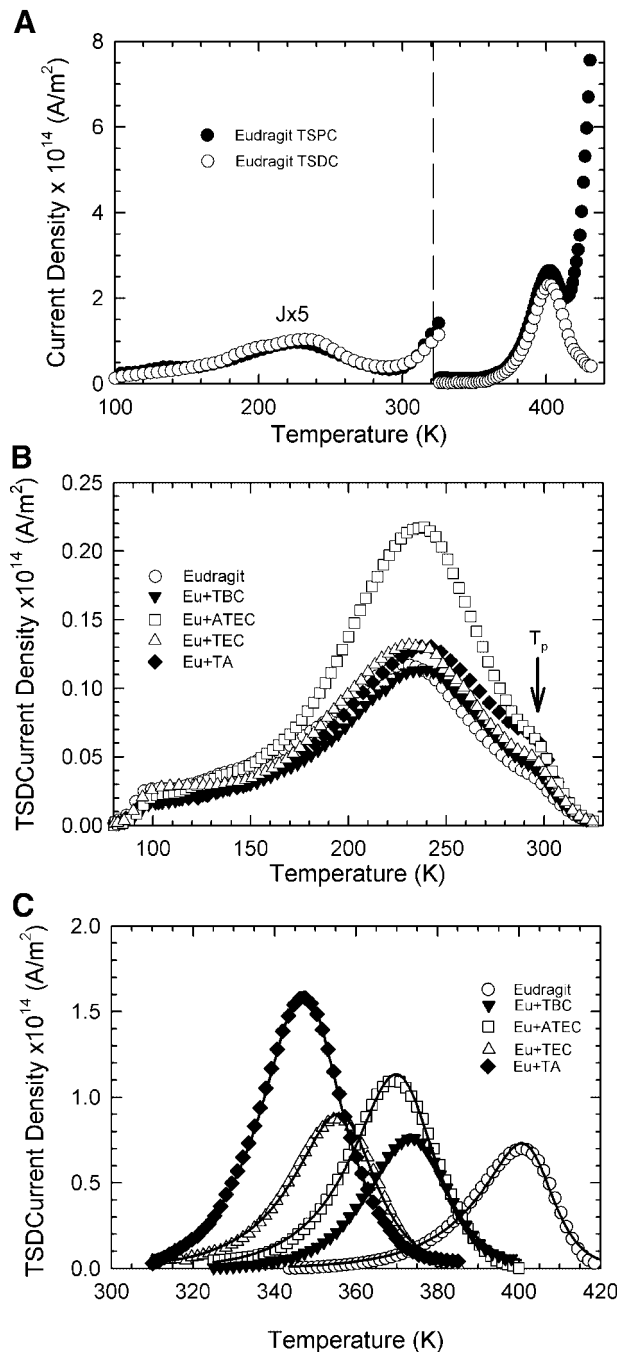


Figure 2. (A) TSPC (filled circles) and TSDC (empty circles) of Eudragit film. (B) Low temperature TSDC spectra of films composed of Eudragit S with and without plasticizers. (C) High temperature TSDC spectra of films composed of Eudragit S with and without plasticizers. The continuous lines are the fitted curves. The density current in (A–C) was normalized to an electric field of 1 V/m.

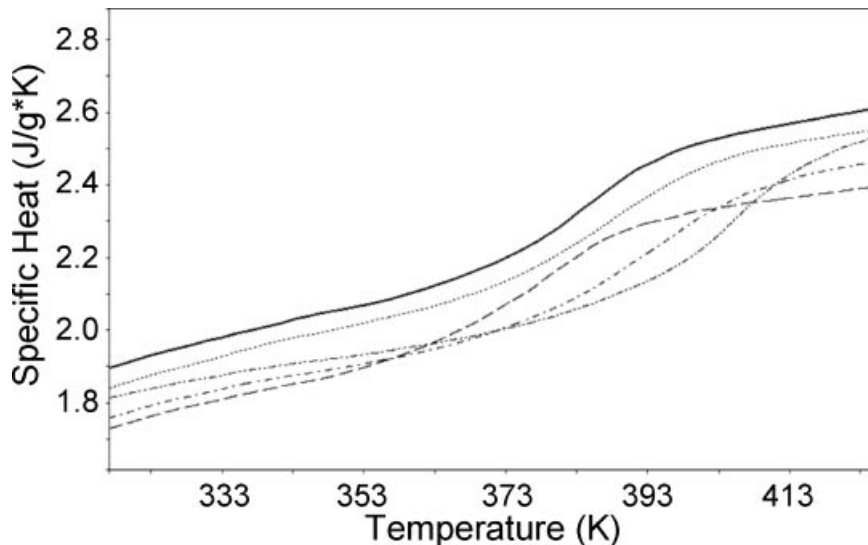


Figure 3. DSC thermograms of Eudragit S with and without plasticizers: — Eu + TEC, ···· Eu + ATEC, --- Eu + TA, - · - · - Eu + TBC, - - - - Eudragit S.

separate the contributions of individual dipolar species to the overall depolarization current that is measured.

The DSA method was applied to the low temperature range (80–310 K) of the TSDC spectra (Fig. 2B) to determine the differences between the secondary relaxations of the films. Representative results of the DSA are shown in Figure 5 for the Eudragit S film. The curve fitting together with the position in temperature and relative contribution of the Debye elementary processes which best fit the data are shown in Figure 5A. The energy window for the best fit ranged from 0.16 to 0.90 eV and the resulting

histogram is shown in Figure 5B. The variation of the pre-exponential factor τ_{0i} corresponding to each energy beam is plotted in Figure 5C.

The pre-exponential factors varied between 10^{-5} and 10^{-13} . The energy histogram was fitted to four mean distributed components, assuming a Gaussian profile for each component. The Gaussian distribution for the reorientation energy has been shown to give the most credible results, and the origin of this energy broadening has been attributed to the electrostatic interactions between dipoles and to contributions from elastic matrix deformations.²¹ The four Gaussian curves, labeled in the order of increasing energy ($\gamma_1, \gamma_2, \beta_1, \beta_2$), are shown in Figure 5B. All the films had these four components in their respective energy histogram. The corresponding mean energies for each peak in the films are listed in Table 3. The mean energy of the γ_1 component remained

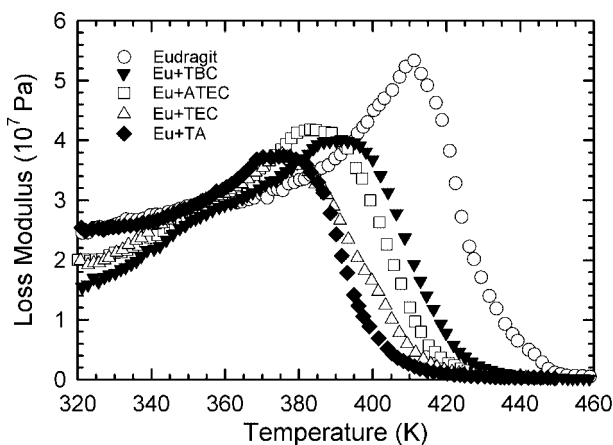


Figure 4. Temperature dependence of loss modulus of Eudragit S with and without plasticizers, at 1 Hz, as obtained from DMA.

Table 2. The Glass Transition Temperatures as Determined by DSC and DMA

Film	T_g (DSC) (K)	T_g (DMA) (K)	Residual Solvent (%)
EU	405.9 ± 0.14	410.8 ± 1.0	1.09 ± 0.22
EU-TBC	394.0 ± 0.94	394.7 ± 2.1	1.65 ± 0.08
EU-ATEC	390.8 ± 2.27	388.5 ± 1.2	1.21 ± 0.16
EU-TEC	383.7 ± 1.03	379.0 ± 0.6	0.63 ± 0.22
EU-TA	377.9 ± 3.62	378.9 ± 1.3	1.10 ± 0.17

The residual solvent in each film is also listed. Mean values \pm SD.

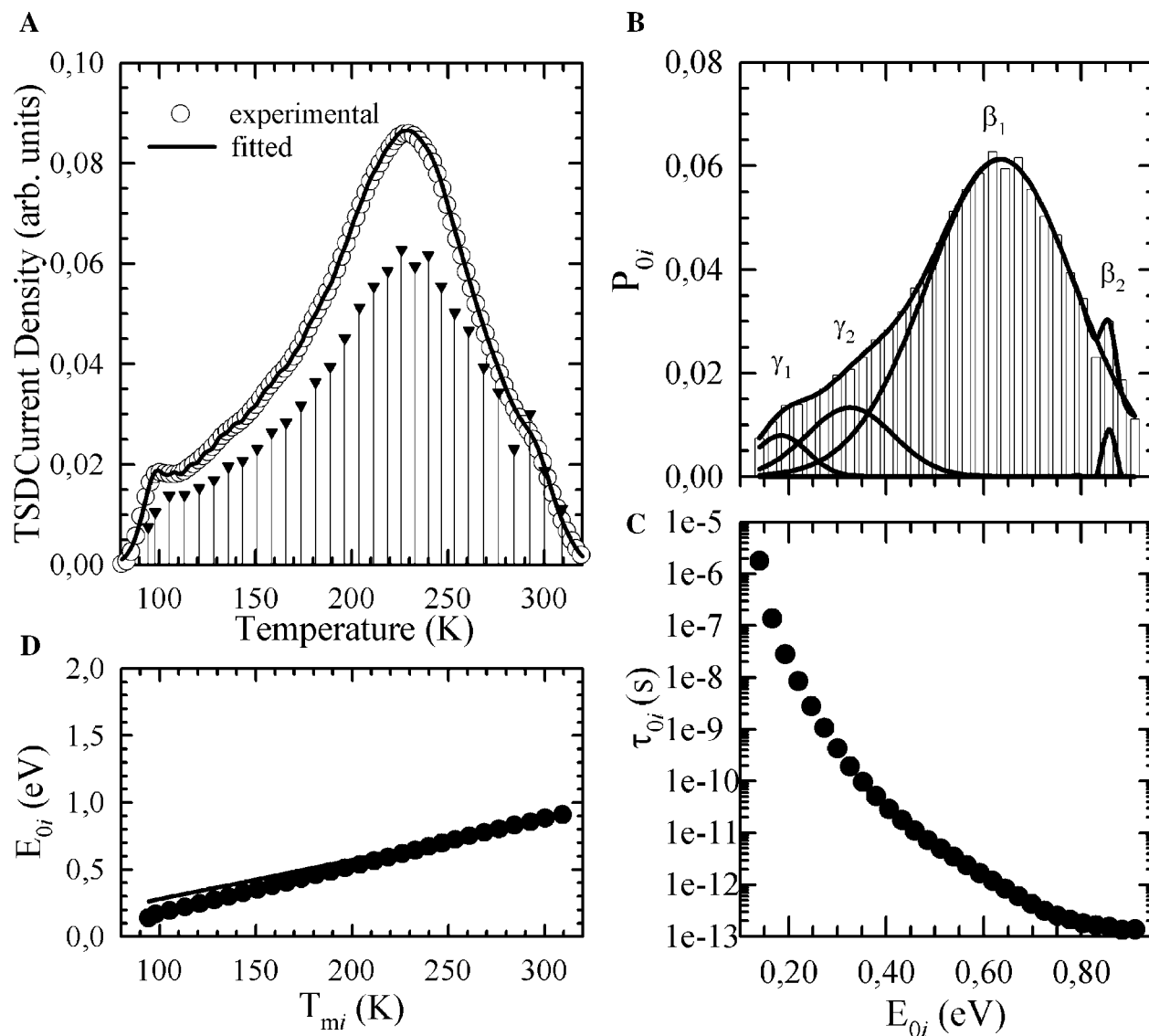


Figure 5. DSA results for the secondary relaxations of Eudragit film. (A) Experimental (empty circles) and fitted (straight line) spectrum. The position in temperature and relative contribution of the Debye elementary processes which best fit the experimental curve are also represented. (B) Energy histogram of the contribution to the polarization of each Debye component peak. (C) Variation of the Arrhenius preexponential factor with the activation energy. (D) Starkweather representation of E_{0i} versus T_{mi} . The filled circles are the DSA results from the numerical decomposition of the secondary relaxations. The line is the zero entropy line.

Table 3. Direct Signal Analysis of the Secondary Relaxations Obtained by TSDC

Sample	$E_{0\gamma_1}(\sigma_{\gamma_1})$ (eV)	$E_{0\gamma_2}(\sigma_{\gamma_2})$ (eV)	$E_{0\beta_1}(\sigma_{\beta_1})$ (eV)	$E_{0\beta_2}(\sigma_{\beta_2})$ (eV)
Eu	0.19 (0.05)	0.33 (0.09)	0.64 (0.15)	0.85 (0.01)
Eu-TBC	0.18 (0.05)	0.37 (0.10)	0.67 (0.13)	0.87 (0.02)
Eu-ATEC	0.19 (0.06)	0.37 (0.10)	0.65 (0.12)	0.85 (0.02)
Eu-TEC	0.18 (0.05)	0.36 (0.10)	0.64 (0.13)	0.85 (0.03)
Eu-TA	0.19 (0.05)	0.37 (0.10)	0.65 (0.15)	0.84 (0.01)

Mean energies (E_0) and width distributions (σ) for each component.

constant in all films at approximately 0.19 eV. However, for the γ_2 component, the energy is significantly higher in the plasticized samples compared to that observed for the Eudragit film alone.

To check that the elementary processes obtained by DSA correspond to local modes of the secondary relaxations, the Starkweather²² representation is presented in Figure 5D. In this figure the zero activation entropy line corresponds to the solution of Eq. (4).

$$E_{0i} = kT_{mi} \left(1 + \ln \left(\frac{kT_{mi}}{2\pi\hbar f_{mi}} \right) \right) \quad (4)$$

The average TSDC equivalent frequency, f_{mi} , is assumed to be 2.47×10^{-3} Hz, and the temperature, T_{mi} , of the elementary peak maxima obtained by DSA is used. The temperature dependence of the activation energies, plotted as filled circles, lies next to the zero-entropy line, with the exception of the first low temperature points that exhibit negative deviation to this line. Some of these contributions belong mainly to the first distributed process (γ_1) that could not be fully reproduced (see Fig. 5B) due to the proximity to the lower temperature limit of our experimental setup. Taking into account this effect, it can be

inferred from the Starkweather representation of Figure 5D that the overall elementary processes obtained by DSC are localized motions with no correlations involved. This trend has been also reported in previous TSDC studies where the decomposition in elementary processes was performed using partial polarization techniques.^{23,24}

The absolute values of each component polarization and the total polarization of the global low temperature band as a function of the dissolution time are calculated and shown in Figure 6. The calculation was made using an electric field strength of 1 V/m. The predominant contribution to the total polarization is from the β_1 component. The γ_1 and β_2 components display the smallest contribution to polarization. The contribution of the γ_2 component is about five times greater than the γ_1 and β_2 components.

As the β_1 and, hence the total secondary relaxations increase, the films display faster dissolution rates. This inverse linear correlation between both the β_1 and the global low temperature peak areas with dissolution time exists for all the films except for the EU-ATEC film. The β_1 component is most likely to be derived from carboxylic acid functional groups (*vide infra*). Facile deprotonation of the carboxylic acid

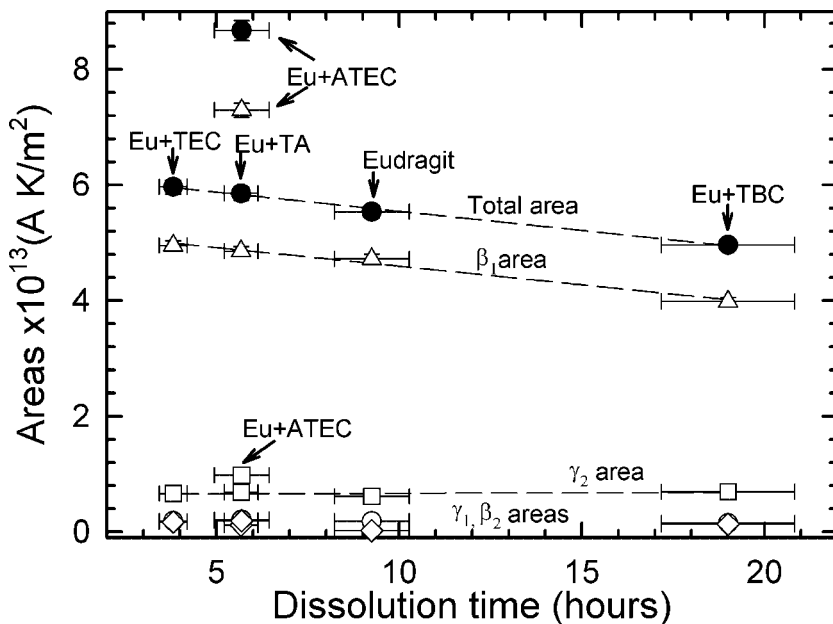


Figure 6. Total polarization of the global low temperature band (filled symbols) and the polarization of each of the four main components (open symbols) vs dissolution onset times of the different Eudragit S films. The dash lines are the best fit to straight lines.

moieties results in ionization which will have a major influence on film dissolution.^{25,26}

Influence of Plasticizers as Determined by Changes in TSDC Secondary Relaxations

Variations in the secondary relaxation caused by plasticizer can arise from changes in local free volume, that is, packing efficiency variations,²⁷ local free volume fluctuations,²⁸ or dynamic interactions and constraints between the polymer and plasticizer.²⁹ Plasticizers can reduce the resistance of polymer molecules to slide past each other by favorably interacting with the polymer through dipolar interactions^{30–32} or other noncovalent interactions, especially hydrogen bonds.³³

Hydrogen bonding with a plasticizer may weaken intermolecular polymer–polymer interactions. This can potentially increase the propensity for water imbibation into the films to facilitate faster dissolution times. The large secondary relaxation area for EU-A TEC may thus contribute to a faster than expected dissolution rate than what would be anticipated by the relative aqueous solubility of the plasticizer.

Structurally TEC and A TEC differ only by the acetylation of the tertiary hydroxyl group in A TEC. This results in A TEC being approximately 10 times less water soluble than TEC. A TEC is a hydrogen bond acceptor only, while TEC is both a hydrogen bond acceptor and donor. Being only a hydrogen bond acceptor, A TEC may interact relatively more efficiently with the carboxylic acid H-bond donors on Eudragit S to reduce polymer–polymer interactions. This relative reduction in polymer–polymer chain interactions results in faster dissolution which cannot be anticipated by the water solubility of A TEC alone.

In a study of the structurally related homopolymer, poly(methyl methacrylate) (PMMA), a small mechanical loss peak was reported¹⁷ and was assigned to the rotation of the methyl groups that are attached directly to the polymer mainchain. This assignment was corroborated by TSDC³³ and nuclear magnetic resonance analysis.³⁴ Ultrasonic attenuation experiments³⁵ indicated an activation energy of about 0.2 eV in the temperature region from 100 to 130 K. These values are similar to the ones found in our work for the γ_1 process. These observations are consistent with the dielectric γ_1 peak of the Eudragit samples being assigned to the orientation of the CH₃ dipoles that are covalently bound to the Eudragit S main chain.

In a series of *n*-alkyl methacrylate polymers examined by McCrum et al.,¹⁷ a γ mechanism was detected by mechanical methods. An activation energy of 0.4 eV, was observed and ascribed to the motions of the pendent ester methyl group. The similar activation energies of this γ process and the γ_2 processes from our study suggest that this reorientation could be assigned to the ester methyl groups in Eudragit S. The increase of the reorientation energy of the γ_2 process in the plasticized film samples compared to the EU control films may be due to the presence of the plasticizer hindering the motions of the ester methyl group.

The broad β_1 component (Tab. 3) suggests that it is a combined process involving a weighted sum of elementary processes occurring in different local environments. A similar β relaxation with an activation energy of 0.7 eV at the same temperature range was observed by mechanical and TSDC techniques for poly(2-chlorocyclohexyl methacrylate).³⁶ This process was attributed to pendent rotations through single bonds linked to the polymer mainchain. The similarity of this β_1 component suggests our observed β_1 peak may also be due to the rotation of the pendent –COOCH₃ and –COOH groups about the C–C bond that links them to the polymer mainchain. As the β_1 area increases, the number of available carboxylic acid functional groups participating in this relaxation becomes larger. Hence the exposed sample must have a greater number of carboxylic acid functional groups that are accessible for ionization by water. This would cause faster dissolution.

Both A TEC and TA are exclusively hydrogen bond acceptors and compete for the carboxylic acid pendent groups in Eudragit S. TA has three ester and A TEC has four ester functionalities, so TA has fewer accepting sites than A TEC. The contribution of other noncovalent interactions between A TEC and Eudragit S should not be disregarded as they can contribute to the large β_1 area of this blend. The molecular volume, shape and polarity of A TEC as well as the accessibility of its carbonyl groups influence its interaction with the polymer.³⁷

The high reorientation energy of the β_2 component (approximately 0.85 eV) is associated with low pre-exponential Arrhenius factors and could be due to overlapping with the low temperature tail of the α transition. It is possible that this relaxation arises from the carbon–carbon bonds along the main chain whose motion would be the initial motions, especially near the chain ends, as

the primary glass transition temperature is approached.

Influence of Plasticizers as Determined by Changes in TSDC Glass Transitions

To better understand the influence of the plasticizer on the dielectric manifestation of the glass transition, the high temperature TSDC profiles were evaluated. An analysis of the α peaks was conducted using the phenomenological model described by Eq. (3). The continuous lines in Figure 2C along with the parameters shown in Table 4 are consistent with the fittings obtained using this analysis.

Our data shows that there is a decrease in the fitted T_g values as the molecular weight of the plasticizer diminishes and its solubility increases (Tabs. 1 and 4). Decreased intermolecular polymer–polymer interactions are also indicated by the higher β parameters (inverse to the peak–width) for the plasticized samples compared to the net film (Tab. 4). Lower T_g values can result because the plasticizers were blended by weight percent rather than by molar percent. For a lower MW plasticizer there are more molecules for a given composition and therefore more molecules are available to occupy the accessible sites along the polymer structure.³⁸ Out of all the plasticizers explored in this study TBC provides the least molecules as it is of the largest MW and included at a lower proportion of polymer weight. The T_g values obtained by DMA and DSC techniques also displayed a tendency to decrease when the molecular weight and the solubility of the plasticizers decreases and increases respectively (Tabs. 1 and 2). This dependency of polymer chain separation and reduction of the intermolecular forces between them on the aqueous solubility of the plasticizer contrasts with the DSC results obtained for the poly(methacrylic acid ethylacrylate) copolymer (Eudragit L100-55) films³⁹ that were plasticized with the same additives as those used in the present work.

Table 4. Analysis of the Glass Transition Relaxations Obtained by TSDC.

Sample	$J_0 \times 10^{11}$ (A/m ²)	β (K ⁻¹)	T_g (K)	η
Eu	0.005	0.0781	404.2	119.6
Eu-TBC	0.0059	0.0968	375.3	95.0
Eu-ATEC	0.0084	0.0864	372.3	88.9
Eu-TEC	0.0066	0.0816	358.6	88.8
Eu-TA	0.0122	0.0969	348.8	83.9

It is interesting to compare the TSDC results obtained with EU-TEC and EU-TBC. These are the fastest and slowest dissolving films respectively. They differ only in the number of carbons in their ester chains (two and four for TEC and TBC respectively). The moieties capable of participating in hydrogen bonds are the same for these two plasticizers with the three ester groups potentially acting as H-bond acceptor sites. The tertiary hydroxyl group has both H-bond donating and accepting character. There is approximately a 19 K difference in the glass transition temperature of the films and a 8 K difference in their global secondary relaxation temperature maxima; with EU-TBC displaying the higher temperature values. It is possible that the butyl alkyl chains of TBC reside more readily between the Eudragit S polymer chains to orient the ester and hydroxyl functional groups with the polar groups on the polymer. This would decrease the local polymer–polymer free volume fluctuations, and consequently cause improved packing; thus facilitating enhanced noncovalent polymer–additive interactions.

Interactions may occur between hydroxyl groups of TBC and H-bond acceptor moieties (e.g., carbonyl in acid and ester groups) of the polymer in addition to interactions of the carbonyl groups of the plasticizer with the H-bond donating moiety (carboxylic acid proton) on the polymer. This latter interaction may explain the increase of the reorientation energy of the β_1 process on EU-TBC and thus the shift to higher temperatures of the global secondary spectrum. Interactions of the carbonyl groups of TBC with the carboxylic acid proton of EU would also decrease the amount of free hydroxyl groups which are accessible to water.³⁸ The combination of low TBC water solubility and increased polar polymer–plasticizer interactions would be consistent with the prolonged dissolution time observed for EU-TBC.

While the T_g of EU-TBC film is lower than that of EU alone (see Tabs. 2 and 4); the trend is not the same when comparing the areas and maxima of the secondary relaxations for the two films. TBC enhances segmental mobility while hindering the mobility of the pendent chain moiety of Eudragit S. These opposing effects of the plasticizer on primary and secondary relaxations of polymer systems has previously been reported by Ngai et al.⁴⁰

Our results show that the T_g values of the polymer films do not correlate to Eudragit S polymer film dissolution; however the secondary

relaxations areas do. From this we can infer that the local environment of the side chains, particularly interactions and free volume fluctuations of the carboxylic acid group, have a predominant effect on polymer film dissolution in comparison to the cooperative mobility of the system.

The relative contribution of plasticizer aqueous solubility and the extent of polymer–polymer interaction disruption on the dissolution of Eudragit S films can be established from a comparison of the dissolution rate of EU-TEC and EU-ATEC films. These two systems displayed relatively small differences in their dissolution times despite an almost 10-fold lower aqueous solubility of ATEC compared to TEC. This suggests that disruption of polymer–polymer interactions can make a significant contribution towards increasing the rate of Eudragit S film dissolution.

Comparison of T_g Values as Determined by DSC, DMA, and TSDC

Determining the T_g by different methods can result in different values being obtained.⁴¹ For comparison, we used three methods to determine the T_g of our isolated polymer films: (1) TSDC, (2) DSC, and (3) DMA. DSC measures the change in specific heat capacity (C_p) of the sample, DMA detects the glass transition *via* mechanical changes, and TSDC detects the T_g through dipolar rearrangements. DSC and DMA are the two most common methods for determining T_g .⁴² DSC measurements give quantitative thermodynamic data for a change in specific heat capacity of the sample at T_g . While only small samples are required, it is sometimes difficult to determine T_g by DSC when it is a minor event⁴² and there are phase separations in a mixture. In contrast, DMA has about 1000 times greater sensitivity for detecting the T_g ¹⁸ however a larger sample size is required.

The T_g values for all the films obtained by TSDC α peaks are listed in Table 4 and those obtained by DMA and DSC are listed in Table 2. All three techniques gave a similar value for Eudragit S films (DSC/DMA:402 K and TSDC: 405.9 K). While the trend was similar for the plasticized films, the T_g values that were obtained by TSDC were lower than the T_g values that were determined by DSC and DMA, which were similar. There was a greater difference between the TSDC and DSC/DMA derived T_g values for the lower

molecular weight plasticizers (TA and TEC). Also the DMA T_g value for EU-TEC was 4.7 K lower than the DSC derived T_g value. Although this difference is relatively small, the data are reproducible with very little variation.

Regarding the difference in the T_g values obtained by TSDC and DSC/DMA, Leroy et al.⁴³ reported a similar observation in their study of poly(vinyl methyl ether/polystyrene) blends. The observed T_g differences between the TSDC and DSC values were rationalized on the basis of the Lodge and McLeish⁴⁴ model (2000) of the “effective concentration” concept. This model links the effective TSDC glass transition temperature to the average segmental mobility of the dielectrically active component in the blend. For a lower MW plasticizer more molecules must be available to occupy the accessible sites along the polymer structure, and consequently the polymer segment will sense greater variations in the effective local concentration. According to the Lodge and McLeish model, this would produce greater differences of the effective local T_g that can be observed by dipolar interactions than the macroscopic T_g obtained by DSC or DMA. Our results are consistent with the predictions of this model.

The correlation of the T_g values obtained by the different methods are plotted in Figure 7. There is a linear correlation between the TSDC and DSC results that is independent of the small differences in residual solvent in each film (Tab. 2).

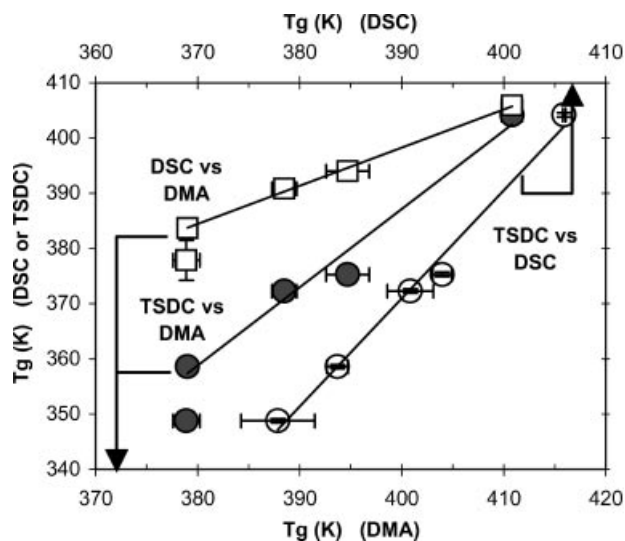


Figure 7. Correlation of T_g 's of the films obtained from the different thermal methods. TSDC T_g versus DMA T_g (filled circles), TSDC T_g versus DSC T_g (empty circles) and DSC T_g versus DMA T_g (empty squares). The lines are the best fit to straight lines.

Additionally, there are two linear relations among the T_g values obtained from TSDC and DSC with respect to that of the DMA, with the exception of the glass transitions of the sample with the smallest plasticizer (EU-TA), which is higher than expected by the linearity shown by the other samples (i.e., the T_g for EU-TA is below the two lines in Figure 7 for TSDC-DMA and DSC-DMA). TA seems to be the most effective plasticizer in interrupting the polymer–polymer interactions, as EU-TA displays the lowest T_g and the highest β -parameter (see Tab. 4). The relatively higher T_g value for EU-TA that was observed by DMA indicates that there are additional plasticizer effects that are manifested in the mechanical relaxations, but not through dielectric and thermal relaxations.

Anderson et al.⁴⁵ studied polystyrene/mineral oil blends and reported the existence of polymer chain end effects that restrict their mobility and thus results in higher moduli and strength than expected. These effects occur when the average diameter of the mineral oil domains was less than or equal to the average size of the free volume voids of the polymer chain ends. In agreement with this result, it could be that as TA is the smallest plasticizer, the chain end effects could affect the mean mechanical relaxation of EU-TA while the dielectric and thermal relaxations could be mainly influenced by the extent of the disruption of polymer-polymer interactions. In Table 1 it can be seen that TA is the only plasticizer that has a tri-substituted carbon. The other plasticizers all have a quaternary carbon. TA has a smaller volume and more mobility due to its tertiary substitution. These characteristics of TA could explain its ability to pack more efficiently at the chain ends of the polymer to restrict chain end mobility. The expectation is that the mechanical relaxations of EU-TA would then decrease. In contrast, the TSDC α peak of EU-TA (Tab. 4) has the highest intensity, smallest width and the lowest T_g . This indicates that the cooperative movements are extended freely along the polymer chain, resulting in disruption of the polymer–polymer interactions in this sample.

CONCLUSIONS

Dissolution of methacrylic acid-methylmethacrylate copolymer films is influenced by the solubility and structure of the citrate plasticizers incorporated in the blend. The detailed analysis of the low

temperature TSDC spectra of the samples provided the means to identify several secondary relaxation mechanisms. Relaxation of the carboxylic acid functional group was identified and its peak area along with the total secondary relaxation peak area were found to be related to the film dissolution times. Secondary relaxation areas are related to polymer plasticizer interactions, and the differences between the films are mainly attributed to hydrogen-bonding. Hydrogen bonding can cause disruption of polymer–polymer interactions which can increase the propensity for water imbibition into the films and can therefore result in an increased dissolution rate. No correlation however was found for the dissolution time of the films with the T_g values obtained by TSDC, DSC and DMA. Polymer–plasticizer interactions have different influences on side chain and segmental relaxations.

The above results indicate that the dielectric secondary relaxations may be a powerful probe to help comprehend the molecular interactions between a plasticizer and a polymer. While this study focused on the interactions between Eudragit S and citrate based plasticizers, our results may contribute towards a better understanding of how noncovalent molecular interactions within a film can influence its dissolution.

ACKNOWLEDGMENTS

The authors thank Mrs Fang Liu for useful discussions and Mr John Gearing at Gearing Scientific for advice on the technical aspects of DMA. GlaxoSmithKline are acknowledged for access to the DMA. M. C. Hernández and N. Suárez are grateful to the Venezuelan National Science Foundation FONACIT for grant G-2005000449, and to the Research and Development Unit (DID) of the Simón Bolívar University (GID-35) for the support given to accomplish this work. This work has also been funded by The School of Pharmacy, University of London.

REFERENCES

1. Basit AW. 2005. Advances in colonic drug delivery. *Drugs* 65:1991–2007.
2. Ibekwe VC, Fadda HM, Parsons GE, Basit AW. 2006. A comparative in vitro assessment of the drug release performance of pH-responsive polymers for ileo-colonic delivery. *Int J Pharm* 308:52–60.
3. Ibekwe VC, Liu F, Fadda HM, Khela MK, Evans DF, Parsons GE, Basit AW. 2006. An investigation

- into the in vivo performance variability of pH responsive polymers for ileo-colonic drug delivery using gamma scintigraphy in humans. *J Pharm Sci* 95:2760–2766.
4. Evans DF, Pye G, Bramley R, Clark AG, Dyson TJ, Hardcastle JD. 1988. Measurement of gastrointestinal pH profiles in normal ambulant human subjects. *Gut* 29:1035–1041.
 5. Fadda HM, Basit AW. 2005. Dissolution of pH-responsive formulations in media resembling intestinal fluids: Bicarbonate vs phosphate buffers. *J Drug Deliv Sci Technol* 15:273–279.
 6. Gotch F, Nadell J, Edelman IS. 1957. Gastrointestinal water and electrolytes. IV. The equilibration of deuterium oxide (D_2O) in gastrointestinal contents and the proportion of total body water (T.B.W.) in the gastrointestinal tract. *J Clin Invest* 36:289–296.
 7. Spiller RC, Brown ML, Phillips SF. 1987. Emptying of the terminal ileum in intact humans—Influence of meal residue and ileal motility. *Gastroenterology* 92:724–729.
 8. Banker GS. 1966. Film coating theory and practice. *J Pharm Sci* 55:81–89.
 9. Lecomte F, Siepmann J, Walther M, Macrae RJ, Bodmeier R. 2004. Polymer blends used for the aqueous coating of solid dosage forms: Importance of the type of plasticizer. *J Control Release* 99:1–13.
 10. Okhamafe AO, York P. 1987. Interaction phenomena in pharmaceutical film coatings and testing methods. *Int J Pharm* 39:1–21.
 11. Jenquin MR, Sarabia RE, Liebowitz SM, McGinity JW. 1992. Relationship of film properties to drug release from monolithic films containing adjuvants. *J Pharm Sci* 81:983–989.
 12. Suarez N, Figueroa D, Laredo E, Puma M. 1982. Thermal depolarization of cubic lead fluoride. *Cryst Lattice Defects* 9:207–210.
 13. Suarez N, Brocchini S, Kohn J. 2001. Study of relaxation mechanisms in structurally related biomaterials by thermally stimulated depolarization currents. *Polymer* 42:8671–8680.
 14. Aldana M, Laredo E, Bello A, Suarez N. 1994. Direct signal analysis applied to the determination of the relaxation parameters from TsdC spectra of polymers. *J Polym Sci Part B Polym Phys* 32:2197–2206.
 15. Puma M. 1997. Phenomenological model to describe the glass transition relaxation peaks for depolarization current experiments. *Polym Adv Technol* 8:39–43.
 16. Sasabe H, Moynihan CT. 1978. Structural relaxation in polyvinyl acetate. *J Polym Sci Part B Polym Phys* 16:1447–1457.
 17. McCrum NG, Read BE, Williams G. 1991. Anelastic and dielectric effects in polymeric solids. New York: Dover.
 18. Chartoff RP. 1997. Thermoplastic polymers. In: Turi EA, editor. *Thermal characterisation of polymeric materials*, 2nd edition. New York: Academic Press. pp. 483–743.
 19. Lippold BC, Pages RM. 2001. Film formation, reproducibility of production and curing with respect to release stability of functional coatings from aqueous polymer dispersions. *Pharmazie* 56:5–17.
 20. Bucci C, Fieschi R. 1964. Ionic thermoconductivity. Method for the investigation of polarisation in insulators. *Phys Rev Lett* 12:16–19.
 21. Laredo E, Puma M, Suarez N, Figueroa DR. 1981. Analysis of the ionic-thermal-current peaks with a distribution in the reorientation energy. *Phys Rev B* 23:3009–3016.
 22. Starkweather HW. 1988. Noncooperative relaxations. *Macromolecules* 21:1798–1802.
 23. Correia NT, Ramos JJM, Descamps M, Collins G. 2001. Molecular mobility and fragility in indomethacin: A thermally stimulated depolarization current study. *Pharm Res* 18:1767–1774.
 24. Ramos JJM, Correia NT, Diogo HP. 2006. TSDC as a tool to study slow molecular mobility in condensed complex systems. *J Non-Cryst Solids* 352:4753–4757.
 25. Spital J, Kinget R. 1979. Solubility and dissolution rate of enteric polymers. *Acta Pharm Technol Suppl* 7:163–168.
 26. Krause S, Mcneil CJ, Armstrong RD, Ho WO. 1997. Behaviour of pH sensitive polymers on metal electrodes. *J Appl Electrochem* 27:291–298.
 27. Shuster M, Narkis M, Siegmann A. 1994. Polymeric antiplasticization of polycarbonate with polycaprolactone. *Polym Eng Sci* 34:1613–1618.
 28. Xiao C, Wu J, Yang L, Yee AF, Xie L, Gidley D, Ngai KL, Rizos AK. 1999. Positronium annihilation lifetime and dynamic mechanical studies of gamma-relaxation in BPA-PC and TMBPA-PC plasticized by TOP. *Macromolecules* 32:7913–7920.
 29. Ngai KL, Rendell RW, Yee AF, Plazek DJ. 1991. Antiplasticization effects on a secondary relaxation in plasticized glassy polycarbonates. *Macromolecules* 24:61–67.
 30. Kirkpatrick A. 1940. Some relations between molecular structure and plasticizing effect. *J Appl Phys* 11:255–261.
 31. Moorshead TC. 1962. Some thoughts on PVC plasticization. In: Kaufman M, editor. *Advances in PVC compounding and processing*. London: Maclaren. pp. 20–31.
 32. Marcilla A, Beltrán M. 2004. Mechanisms of plasticizer action. In: Wypych G, editor. *Handbook of plasticizers*. Toronto: ChemTec Publishing. pp. 106–125.
 33. Wu C, McGinity JW. 2003. Influence of methylparaben as a solid-state plasticizer on the physico-

- chemical properties of Eudragit[®] RS PO hot-melt extrudates. *Eur J Pharm Biopharm* 56:95–100.
34. Matsuoka S, Ishida Y. 1966. Multiple transitions in polycarbonate. *J Polym Sci Part C Polym Symp* 14:247–259.
 35. Tanabe Y, Hirose J, Okano K, Wada Y. 1970. Methyl group relaxations in the glassy phase of polymers. *Polymer J* 1:107–115.
 36. Sanchis MJ, Calleja RD, Gargallo L, Hormazabal A, Radic D. 1999. Relaxational study of poly(2-chlorocyclohexyl methacrylate) by thermally stimulated current, dielectric, and dynamic mechanical spectroscopy. *Macromolecules* 32:3457–3463.
 37. Tarvainen M, Sutinen R, Somppi M, Paronen P, Poso A. 2001. Predicting plasticization efficiency from three-dimensional molecular structure of a polymer plasticizer. *Pharm Res* 18:1760–1766.
 38. Mathew AP, Dufresne A. 2002. Plasticized waxymaize starch: Effect of polyols and relative humidity on material properties. *Biomacromolecules* 3:1101–1108.
 39. Gutierrezrocca JC, McGinity JW. 1994. Influence of water-soluble and insoluble plasticizers on the physical and mechanical-properties of acrylic resin copolymers. *Int J Pharm* 103:293–301.
 40. Ngai KL, Rendell RW, Yee AF, Plazek DJ. 1991. Antiplasticization effects on a secondary relaxation in plasticized glassy polycarbonates. *Macromolecules* 24:61–67.
 41. Georgoussis G, Kyritsis A, Bershtein VA, Fainleib AM, Pissis P. 2000. Dielectric studies of chain dynamics in homogeneous semi-interpenetrating polymer networks. *J Polym Sci Part B Polym Phys* 38:3070–3087.
 42. Sircar AK, Galaska ML, Rodrigues S, Chartoff RP. 1999. Glass transition of elastomers using thermal analysis techniques. *Rubber Chem Technol* 72:513–552.
 43. Leroy E, Alegria A, Colmenero J. 2002. Quantitative study of chain connectivity inducing effective glass transition temperatures in miscible polymer blends. *Macromolecules* 35:5587–5590.
 44. Lodge TP, Mcleish TCB. 2000. Self-concentrations and effective glass transition temperatures in polymer blends. *Macromolecules* 33:5278–5284.
 45. Anderson SL, Grulke EA, Delassus PT, Smith PB, Kocher CW, Landes BG. 1995. A model for antiplasticization in polystyrene. *Macromolecules* 28:2944–2954.